# Air-to-Ground Channel Characterization for Unmanned Aerial Vehicles Based on Field Measurements in 5G at 3.5 GHz

Lucas Val-Terrón
*Gradiant*
Vigo, Spain

J. Joaquín Escudero-Garzás
*Gradiant*
Vigo, Spain

Luis Pérez-Roca
*Gradiant*
Vigo, Spain

Ana María Vega-Viejo
*Telefónica España*
Madrid, Spain

Ángel Alves-González
*Telefónica España*
Madrid, Spain

***Abstract*—The last years have seen an unprecedented interest in the utilization of aerial platforms not only to support applications (e.g. monitoring) but also to assist in relaying signals from terrestrial networks. In this new paradigm, it is capital to have an estimation of the communication channel, which is quite different from the terrestrial channel. This paper presents a channel model for air-to-ground (A2G) communications based on a measurement campaign over an in-service 5G NSA (non-standalone) network, whic allows for future investigations to have an estimate of the path loss in similar environments, and provides a full detail of the measurements**

***Index Terms*—Unmanned Aerial Vehicles (UAV), Measurement, Channel model, Path loss, Air-to-ground.**

## I. Introduction

Historically, non-terrestrial networks (NTN), including satellites and flying platform stations, have evolved with little interaction with terrestrial networks. This perspective radically changed in the last two 3GPP releases, which consider the integration of terrestrial and NTNs as inherent to the 5G "network of networks" [1] and its evolution towards 6G. In particular, UAVs have become a component of mobile networks, shifting their role from military scenarios [2] to civilian applications such as surveillance or search and rescue operations [3]. Beyond their utilization for final-user applications, UAVs have recently shown their potential as network nodes. Indeed, UAVs may enable coverage extension to remote access areas [4] and the support of aerial cellular networks [5].

In wireless communications systems, it is essential to have information on the propagation environment so that both transmitter and receiver can adapt the transmission and reception processes to those effects introduced by the channel. Therefore, research efforts to characterize the air-to-ground (A2G) channel has increased in the last years to achieve reliable A2G communications. The measurement-driven study of [6] leads to the characterization of wireless channels between UAV platforms and terrestrial users for cellular (900 MHz and 1800 MHz) and WiFi (5 GHz) frequency bands in terms of path loss. In [7], the authors propose an empirical channel model that includes the variation of different parameters (e.g., the path loss exponent) with the UAV height for LTE at 2.585 GHz in an experimental setting based on Universal Software Radio Peripheral (USRP) devices. More recently, the work of [8] presents a wideband characterization of A2G channels in terms of Rician $K$-factor and root mean squared (RMS) delay spread based on multienvironment channel measurements with a center frequency of 6.5 GHz and bandwidth of 500 MHz. From a theoretical perspective, the authors of [9] propose a 3D non-stationary geometry-based stochastic model for UAV-to-ground multiple-input-multiple-output (MIMO) channels to support the future UAV-integrated 6G networks. However, as evidenced in [10], little attention has been devoted to modelling low altitude A2G channels compared to the existing literature in other UAV communication modalities.

This work contributes to the state of the art in A2G communication modelling with the characterization of the uplink by means of field measurements in horizontal UAV flights at different heights. The monitored communication channel is established between a in-service 5G

978-1-6654-6975-3/22/$31.00 ©2022 IEEE

NSA (non-standalone) base station (eNB) and the UAV. Then, the model is valid for any similar transmission in the licensed frequency of 3.5 GHz. Besides, due to regulatory and battery restrictions, UAVs are expected to operate within a limited range and low altitudes, being both factors present in our measurement campaign.

This paper is organized as follows. Section II presents the A2G channel model, Section III describes the measurements environment and specifications, and Section IV shows the results after processing the field measurements. We give our conclusions in Section V.

## II. UAV CHANNEL MODEL

For channel characterization, we propose the use of the floating intercept model, or alpha-beta model, used in the WINNER II and 3GPP channel models [11]. This model fits the best line to the measured data via a regression to create a floating intercept linear equation model:

$$\text{PL[dB]} = \alpha + \beta \log_{10} d + X_\sigma, \qquad (1)$$

where PL stands for the path loss in dB, $\alpha$ is the intercept in dB, $\beta$ represents the slope of the fitting line, and $X_\sigma$ is a zero-mean Gaussian random variable with standard deviation $\sigma$ in dB. In this paper, the objective is to characterize the path loss in (1) from the measurements obtained in a suburban area (see Section III). In particular, we extract the values of $\alpha, \beta,$ and $X_\sigma$ for different altitudes and distances.

The parameters $\alpha, \beta$ provides a characterization of the path loss (no shadowing component) for the environment of Section III. These parameters respond to the best fitting curve for the set of measurements in terms of path loss. $X_\sigma$ characterizes the shadowing effect with $h$, obtained as follows [12]:

1) For each $h$ at a distance $d$, we obtain $N$ measurements to calculate the average received power $\bar{P}_r$.
2) A set of $N$ values $X_\sigma(n) = \bar{P}_r - P_r(n)$ provides the estimated shadowing for the pair $(h, d)$, where $P_r(n)$ is the received power at the $n$th measurement.
3) The distribution of $X_\sigma(h)$ given by the by all the values $X_\sigma(n), n = 1, \ldots, N$.

## III. MEASUREMENTS ENVIRONMENT AND SPECIFICATIONS

This section details the measurement hardware equipment, the eNB specifications, a complete description of the scenario and the measurements methodology.

### A. Measurement hardware equipment

As Fig.1 illustrates, the hardware equipment used to perform 5G NSA signal measurements is composed of two parts, the ground segment and the air segment. The ground segment consists of a laptop computer and a drone radio controller. The laptop computer deploys a flight planning software used to automatize the control of the drone, guiding it through the measurement routes previously defined. Control orders from the flight planner are bypassed to the drone radio controller using a Wi-Fi hotspot. Both communications links, Wi-Fi hotspot and drone proprietary link, transmit in ISM 5.8 GHz and 2.4 GHz bands, which guarantee not to interfere with the 5G NSA 3.5 GHz band sensed in this study. The air segment (Fig.2) integrates in a quadcopter drone (DJI Matrice 210) a 5G smartphone Xioami Mi 10 compatible with both 5G NSA and 5G SA bands. In addition, the smartphone is equipped with a license of Tems Pocket 22, a phone-based test tool used to track the quality parameters of the network.

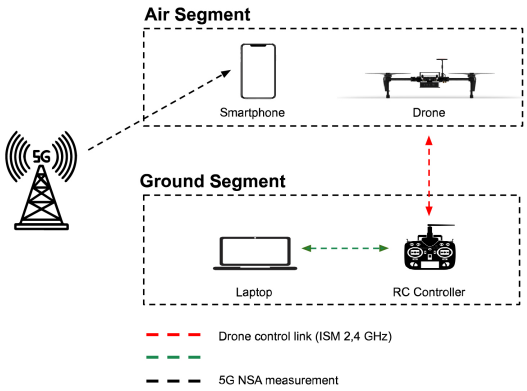


Fig. 1. Measurement equipment diagram.


Fig. 2. Air segment equipment.

### B. 5G NSA eNB specifications

For field measurements, a 5G NSA eNB from Nokia was sensed with Tems Pocket deployed on a Xiaomi Mi 10 5G. The radio specifications of the eNB are detailed

in Table I. The node antennas consists of 5G adaptive antenna systems with 64T64R digital beamforming for multi-user MIMO. Fig.3 reveals the horizontal and vertical radiation pattern of the antennas.

TABLE I
5G NSA ENB SPECIFICATIONS, NOKIA AIRSCALE AEQE MAA 64T64R 192AE ANTENNA

| Parameters | Value |
|---|---|
| EIRP (dBm) | 71.48 |
| Band | n78 |
| Central Freq (MHz) | 3549.99 |
| BW (MHz) | 100 |
| Duplex Mode | TDD |

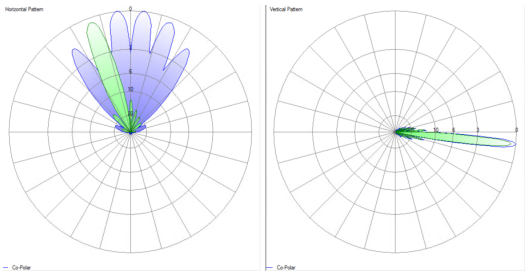

Fig. 3. Antenna radiation diagram.

### C. Measurements scenario and methodology

The measurements were conducted in a suburban area near the center of Segovia, Spain. The scenario is characterized by the basin of a river, surrounded only by very low-lying vegetation and small houses. At the deepest point of the basin, a slope of about 50 meters height is registered. As the eNB is located at the top of the hill with a height of about 30 meters, LoS is guaranteed through all the route. The eNB keeps the same original configuration for terrestrial coverage mainly, as it has not been optimized specifically for UAV flight.

Regarding the measurements methodology (see Fig.4), three non consecutive horizontal flights of 700 meters from the eNB were conducted at heights of 10, 20, 30, 40, 60, 80, 100 and 120 meters. Furthermore, to compensate the variability of the quality measurements registered, stops of 30 seconds were done at each 100 meters step from the eNB (100, 200, 300, 400, 500, 600, and 700 meters), though this setup is limited by the autonomy of the drone used. During this operation, the Tems Pocket application continuously recorded the netowrk quality parameters (RSRP, RSSI, RSRQ, SINR and CID) in an interval of about 1 second, which leads to more than 90 measurements per point of study.

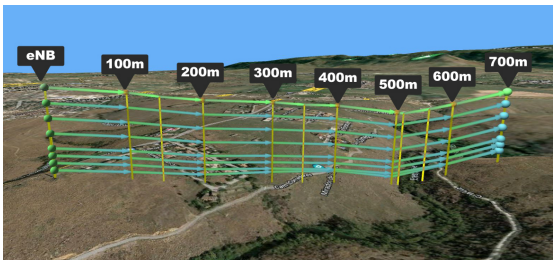


Fig. 4. Measurement flight routes.

## IV. RESULTS

As detailed in Section II, the shadowing distribution is obtained from the field measurements. The resulting distribution is a zero-mean (or almost zero-mean) Gaussian distribution with standard deviation $X_h$ (see Fig.5 as an example for $h = 10m$). The values corresponding to the different heights are shown in Table II. We observe that there exists a trend to keep the shadowing around 4, with no clear inclination to increase or decrease with *h*, as it is also reported in [7]. Other studies confirm this trend, with a slight increase [13] or decrease [14]. The only exception is the value of 1.78 for $h = 10$m, which is well below the other values. Our hypothesis is that the number of samples is insufficient for this case, as the measured power is higher than for other heights.

The parameters that characterize the path loss $(\alpha, \beta)$ are obtained by fitting the measurement points to the best curve (see Fig.6 as an example for $h = 10m$). These curves allow to estimate the path loss in those environments similar to the scenario presented in Section III. The values corresponding to the different heights are shown in Table III.

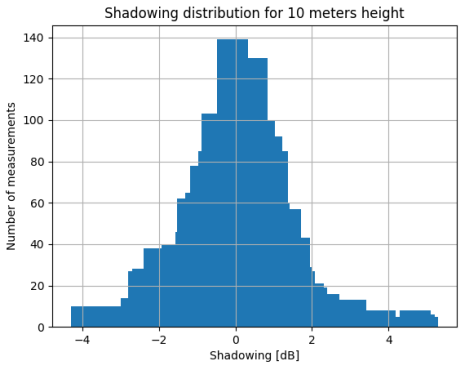


Fig. 5. Shadowing histogram with the measurements for 10-meter height.

TABLE II
SHADOWING PER HEIGHT

| **Height (meters)** | $X_h$ **(dB)** |
|---|---|
| 10 | 1.78 |
| 20 | 4.00 |
| 30 | 3.18 |
| 40 | 4.73 |
| 60 | 3.76 |
| 80 | 3.73 |
| 100 | 4.72 |
| 120 | 4.47 |

TABLE III
PATH LOSS PARAMETERS

| **Height (meters)** | $\alpha$ | $\beta$ |
|---|---|---|
| 10 | 133.15 | 7.73 |
| 20 | 124.01 | 8.75 |
| 30 | 76.17 | 27.98 |
| 40 | 139.74 | 3.48 |
| 60 | 138.00 | 7.64 |
| 80 | 131.79 | 10.92 |
| 100 | 149.41 | 3.98 |
| 120 | 137.51 | 8.39 |

## V. CONCLUSIONS

This paper presents the characterization of the A2G communication channel based on field measurements from an in-service 5G SA network. With the logical differences due to the scenarios, the estimates of path loss and shadowing agree with the trends that can be found in the recent literature.

## ACKNOWLEDGMENT

This work is part of the "Piloto 5G Galicia" project, promoted by the Ministry of Economic Affairs and Digital Transformation through Red.es, and co-funded by the European Regional Development Fund (ERDF) to develop 5G technology in Spain, under grant 00075793.

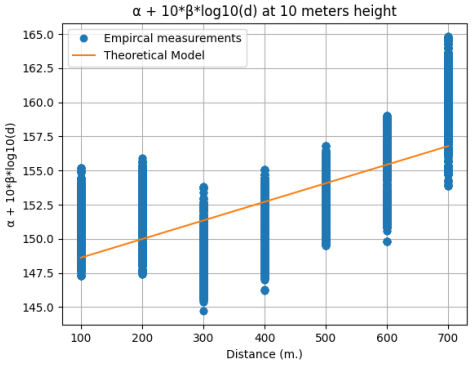


Fig. 6. Path loss characterization for $h = 10$m

## REFERENCES

[1] TR 21.917 Release 17 Description; Summary of Rel-17 Work Items, V0.6.0, June 2022.

[2] Y. Zeng, R. Zhang, and T. J. Lim, "Wireless communications with unmanned aerial vehicles: opportunities and challenges," *IEEE Communications Magazine*, vol. 54, no. 5, pp. 36–42, 2016.

[3] H. Shakhatreh, A. H. Sawalmeh, A. Al-Fuqaha, Z. Dou, E. Almaita, I. Khalil, N. S. Othman, A. Khreishah, and M. Guizani, "Unmanned aerial vehicles (UAVs): A survey on civil applications and key research challenges," *IEEE Access*, vol. 7, pp. 48 572–48 634, 2019.

[4] Q. Yuan, Y. Hu, C. Wang, and Y. Li, "Joint 3D Beamforming and Trajectory Design for UAV-Enabled Mobile Relaying System," *IEEE Access*, vol. 7, pp. 26 488–26 496, 2019.

[5] A. S. Abdalla, A. Yingst, K. Powell, A. Gelonch-Bosch, and V. Marojevic, "Open Source Software Radio Platform for Research on Cellular Networked UAVs: It Works!" *IEEE Communications Magazine*, vol. 60, no. 2, pp. 60–66, 2022.

[6] Y. Shi, R. Enami, J. Wensowitch, and J. Camp, "Measurement-based characterization of LOS and NLOS drone-to-ground channels," in *2018 IEEE Wireless Communications and Networking Conference (WCNC)*, 2018, pp. 1–6.

[7] X. Cai, J. Rodríguez-Piñeiro, X. Yin, N. Wang, B. Ai, G. F. Pedersen, and A. P. Yuste, "An Empirical Air-to-Ground Channel Model Based on Passive Measurements in LTE," *IEEE Transactions on Vehicular Technology*, vol. 68, no. 2, pp. 1140–1154, 2019.

[8] Z. Cui, C. Briso-Rodríguez, K. Guan, I. Guvenç, and Z. Zhong, "Wideband Air-to-Ground Channel Characterization for Multiple Propagation Environments," *IEEE Antennas and Wireless Propagation Letters*, vol. 19, no. 9, pp. 1634–1638, 2020.

[9] H. Chang, C.-X. Wang, Y. Liu, J. Huang, J. Sun, W. Zhang, and X. Gao, "A novel nonstationary 6g uav-to-ground wireless channel model with 3-d arbitrary trajectory changes," *IEEE Internet of Things Journal*, vol. 8, no. 12, pp. 9865–9877, 2021.

[10] C. Yan, L. Fu, J. Zhang, and J. Wang, "A comprehensive survey on uav communication channel modeling," *IEEE Access*, vol. 7, pp. 107 769–107 792, 2019.

[11] T. S. Rappaport, G. R. MacCartney, M. K. Samimi, and S. Sun, "Wideband Millimeter-Wave Propagation Measurements and Channel Models for Future Wireless Communication System Design," *IEEE Transactions on Communications*, vol. 63, no. 9, pp. 3029–3056, 2015.

[12] R. He, Z. Zhong, B. Ai, J. Ding, Y. Yang, and A. F. Molisch, "Short-term fading behavior in high-speed railway cutting scenario: Measurements, analysis, and statistical models," *IEEE Transactions on Antennas and Propagation*, vol. 61, no. 4, pp. 2209–2222, 2012.

[13] J. Rodríguez-Piñeiro, T. Dominguez-Bolaño, X. Cai, Z. Huang, and X. Yin, "Air-to-ground channel characterization for low-height uavs in realistic network deployments," *IEEE Transactions on Antennas and Propagation*, vol. 69, no. 2, pp. 992–1006, 2021.

[14] R. Amorim, H. Nguyen, P. Mogensen, I. Z. Kovács, J. Wigard, and T. B. Sørensen, "Radio channel modeling for uav communication over cellular networks," *IEEE Wireless Communications Letters*, vol. 6, no. 4, pp. 514–517, 2017.